Jordan Journal of Physics

ARTICLE

First Principles' Calculations of CO Adsorption on Bimetallic Nickel-Iron Clusters

Muna Tayyem[a], **Bothina Hamad**[b,c] and **Abdel-Monem M. Rawashdeh**[a]

[a] *Department of Chemistry, Yarmouk University, Irbid, 21163 Jordan.*
[b] *Department of Physics, The University of Jordan, Amman 11942, Jordan.*
[c] *Department of Physics, The University of Arkansas, Fayetteville, AR 72701, USA.*

Abstract: Density functional theory (DFT) calculations using the Generalized Gradient Approximation (GGA) functional are performed to investigate the structural, energetic and magnetic properties of bimetallic alloyed Ni_nFe_{N-n} isomers (N = 2-6 and N = 43, n = 0 to N). The negative mixing energies indicate the stability of these clusters as compared to Ni and Fe bare clusters. All clusters exhibit high spin ground states, with a significant decrease in the magnetization per atom for $Fe_{19}Ni_{24}$ cluster with the iron core. The adsorption energies of CO on the most stable isomers of alloyed clusters are lower than those on Fe clusters with the same structure. This behavior indicates a decrease of CO poisoning and an increase of methanol oxidation reaction (MOR) activity upon alloying.

Keywords: Ni-Fe bimetallic clusters, DFT, CO adsorption, Methanol oxidation reaction, Catalytic activity.

1. Introduction

Bimetallic clusters have chemical and physical properties that are different from those of bulk bimetals. These properties depend on cluster size and composition [1]. Therefore, several experimental [2–5] and theoretical studies [6–8] have been conducted to investigate the properties of such bimetallic clusters. They have been widely used as catalysts, such as Au-Cu [9–11], Au-Pt [12–15], Au-Pd [16–19], Pt-Sn [20–22], Pt-Ru [23–26], Pt-Pd [27–32] and Ag-Pd [33–35]. Bimetallic nickel and iron nanoparticles have been recognized experimentally as heterogeneous catalysts for methanol oxidation reaction (MOR) [36]. Carbon monoxide is the main poisoning species in MOR process, since it adsorbs to the active sites of the catalytic nanoparticles [37–40]. For example, Pt catalysts, which are widely used in industrial reactions, such as MOR, are poisoned by CO adsorption. Therefore, alloying with other metals decreases the adsorption energy of CO on the surface of Pt nanoparticles while preserving the catalytic activity [40]. In addition, Ni-Fe nanoparticles are promising catalysts for MOR [36]. Thus, thorough investigations are required to understand the effect of using bimetallic Ni-Fe nanoclusters as catalysts to decrease CO poisoning that in turn enhances MOR activity.

In spite of the significance of CO adsorption on Ni-Fe nano-particles, yet theoretical investigations are scarce. Cluster expansion (CE) method and coarse grained model were used to investigate the geometrical structure of Ni-Fe nano-particles and the adsorption of CO on Ni-Fe nano-clusters, which include 147 and 150 atoms [41]. Furthermore, the adsorption of CO on the FeNi(111) surface has been studied using the DFT method [42]. The above-mentioned studies present the adsorption of CO on relatively very large clusters using coarse

---

Corresponding Author: Muna Tayyem   **Email**: tayyoom@gmail.com, muna.tayyem@yu.edu.jo

grained model or the adsorption on a surface. Up to our knowledge, there are no computational studies on the effect of alloying on the adsorption energy of CO on relatively small-sized atomistic Ni-Fe clusters. This study provides a clear insight into the effect of composition and atomic configuration on the adsorption energy and therefore catalytic activity of these alloyed Ni-Fe clusters. Furthermore, there are no studies on the catalytic effect of alloyed Ni-Fe clusters compared to bare Ni and Fe clusters. In this work, DFT calculations are performed to determine the structural stability and magnetic properties of small-sized Ni-Fe clusters as an initial step to specify the most stable Ni-Fe clusters in order to study the adsorption of CO on these most stable Ni-Fe clusters.

2. Methodology

The calculations were performed using spin-polarized DFT calculations [43] within the Generalized Gradient Approximation (GGA) of Perdew-Burke-Ernzerhof (PBE) [44] as implemented in Quantum Espresso code [45]. A plane wave basis was set and ultra-soft pseudopotentials for PBE calculations were used to describe the ionic cores within the scalar-relativistic description. Methfessel-Paxton smearing [46] was applied for a better convergence with a smearing width of 0.2 eV. Convergence tests were performed to find the sufficient cut-off energy, where the error in total energy is ±5 meV. The used cut-off energy is 476 eV and the calculations are performed at the gamma Γ-point. The clusters were placed at the center of cubes (18.5 Å for the clusters between n = 2 and 6 and 26.5 Å for n = 43). The dimensions of the cube are tested to achieve isolation of the cluster. Structural optimization is performed with Broyden-Fletcher-Goldfarb-Shanno (BFGS) method.

The stability of heterogeneous clusters is compared with respect to their composition by calculating the mixing energy using Eq. (1).

$$E_{mix} = \frac{1}{N}\left[E_{Ni_nFe_{N-n}} - \frac{n}{N}E_{Ni_N} - \left(\frac{N-n}{N}\right)E_{Fe_N}\right] \quad (1)$$

where, E_{mix}, N, n, $E_{Ni_nFe_{N-n}}$, E_{Ni_N} and E_{Fe_N} are the mixing energy per atom, total number of atoms in the cluster, number of Ni atoms, total energy of bimetallic cluster, energy of bare Ni cluster that has N atoms and energy of bare Fe cluster that has N atoms, respectively. The adsorption energy of CO on Ni-Fe bimetallic cluster is calculated using the following equation:

$$E_{ads} = -\left[E_{Ni_nFe_{N-n}CO} - E_{Ni_nFe_{N-n}} - E_{CO}\right] \quad (2)$$

where, $E_{Ni_nFe_{N-n}CO}$, $E_{Ni_nFe_{N-n}}$ and E_{CO} are the total energy of $Ni_nFe_{N-n}CO$ system, the total energy of bimetallic cluster and the energy of isolated CO, respectively.

3. Results and Discussion

This section presents the results of optimized Ni_nFe_{N-n} clusters with different sizes (N = 2 to 6 and N = 43, n = 0 to N) and compositions. The magnetic properties of Ni-Fe dimer are studied to verify the validity of the used method. In addition, the structural stability with respect to their compositions and magnetic properties is investigated.

The adsorption of CO on most of the stable small-sized Ni-Fe clusters (N = 2 to 6) as well as on the large cluster (N = 43) is investigated. The results of these investigations are compared with the adsorption of CO on bare Ni and bare Fe clusters.

3.1 Ni-Fe Dimer

The bond length, dissociation energy De and the total magnetic moment of Ni-Fe dimer are presented in Table 1. The bond length of this dimer is found to be 2.03 Å, in agreement with other calculations of 2.06 Å [47] and 2.08Å [48] using the linear combination of atomic orbitals (LCAO), the discrete variational (DV-Xa) method and the first-principles' molecular-orbital (MO) approach, respectively. In addition, the obtained dissociation energy De is found to be 1.55 eV/atom, which is close to the value obtained by Cheng and Ellis of 1.39 eV/atom [47]. The obtained total magnetic moment is 5.05 μB, which is slightly higher than the value obtained by Cheng and Ellis [47] and Nakazawa [49] of 5.0 μB.

TABLE 1. The bond length, dissociation energy De, and total magnetic moment of Ni-Fe dimer.

Study	Bond length (Å)	De (eV/atom)	Total magnetic moment (μ_B)
GGA[a]	2.03	1.55	5.05
UB3LYP/LanL2DZ [b]	2.34	1.04	5.00
LCAO DV-Xa[c]	2.06	1.39	5.00
MO[d]	2.08	2.33	3.00

[a] present work.
[b] Ref.[49], [c] Ref.[47], [d] Ref.[48].

3.2 Ni_nFe_{N-n}(N = 3 to 6 and N = 43) Clusters

This sub-section presents the calculations of Ni_nFe_{N-n}(N = 3 to 6 and N = 43, n = 0 to N) clusters. The stability of heterogonous clusters with respect to their compositions is determined by calculating the mixing energy per atom for each composition. The mixing energy is used previously by Sahoo [50] to investigate the stability of binary clusters. The mixing energy per atom for small-sized Ni-Fe clusters with N = 3 to 6 is shown in Fig. 1 to Fig. 3. The mixing energies are found to be negative due to the lower energy values of Ni_nFe_{N-n} clusters as compared to the corresponding Ni and Fe bare clusters. This indicates that alloyed clusters are more stable than bare clusters, in agreement with a previous study by Sahoo et al. [50]. The most stable isomers are shown in Table 2 based on the value of mixed energy. All possible configurations were optimized for Ni_nFe_{N-n} (N = 3 and 4) clusters. The most stable composition of Ni_nFe_{3-n} cluster is Fe$_2$Ni with C$_{\infty v}$ symmetry. This finding is in agreement with the results obtained by Nakazawa et al. [49]. The calculated magnetic moment per atom for this composition is 2.67 µB/atom, which is higher than that obtained by Nakazawa et al. of 2.33 µB/atom [49]. On the other hand, the bond lengths of Fe-Fe and Fe-Ni bonds are 2.13 Å and 2.09 Å, respectively, which are lower than those obtained by Nakazawa et al. of 2.39 Å and 2.37 Å, respectively [49]. These differences in the values of magnetic moment and bond length are due to the use of a different functional (UB3LYP/LanL2DZ) [49]. The most stable composition of Ni_nFe_{4-n} clusters is Fe$_2$Ni$_2$ with D$_{2h}$ rhombus shape, which was not tested by Nakazawa et al. who only optimized square and tetrahedral shapes [49]. All the possible compositions of trigonal bipyramidal and octahedron shapes were investigated for Ni_nFe_{5-n} and Ni_nFe_{6-n} clusters, respectively. The most stable compositions for the cases of Ni_nFe_{5-n} (trigonal bipyramidal shape) and Ni_nFe_{6-n} (octahedron shape) clusters are Fe$_2$Ni$_3$ and Fe$_2$Ni$_4$ with C$_{2v}$ symmetry. These results are consistent with those of Nakazawa et al. [49], where the C$_{2v}$ symmetry was found to be more stable than D$_{3h}$ and D$_{4h}$ symmetries. According to Nakazawa et al. [49], Fe$_2$Ni$_3$ with C$_{2v}$ symmetry (binding energy = 1.48 eV/atom) is more stable than D$_{3h}$ symmetry (binding energy = 1.44 eV/atom). In addition, Fe$_2$Ni$_4$ with C$_{2v}$ symmetry (binding energy = 1.68 eV/atom) is more stable than D$_{4h}$ symmetry (binding energy = 1.65 eV/atom). Thus, the preferred positions of Fe atoms in Ni_nFe_{5-n} and Ni_nFe_{6-n} clusters are the equatorial sites of trigonal bipyramidal and the octahedron, respectively, which increases the number of Fe-Fe bonds, in agreement with Sahoo et al. [50]. A larger Fe-Ni cluster with N= 43 is chosen to study the effect of size on the structural and magnetic properties. According to previous theoretical [41,50,51] and experimental [52] results, Fe atoms prefer the core region of the Fe-Ni cluster, while Ni atoms prefer the surface. It was previously demonstrated that our fcc Fe$_{19}$Ni$_{24}$ cluster is the most stable structure [51]. We found that the Fe-Fe bond length ranges from 2.56 to 2.63 Å, which is close to the value obtained by Guirado-López [51] of 2.7 Å.

All possible compositions of i_nFe_{N-n} (N = 3 to 6 and N = 43, n = 0 to N) clusters were investigated and the most stable clusters are presented in Table 2. All studied Ni-Fe clusters exhibit high spin ground state (Table 2). However, there is a decrease in the value of the total magnetic moment per atom (1.73 µB/atom) for the large Fe$_{19}$Ni$_{24}$ cluster in comparison with small-sized clusters (N= 3 to 6), see Table 2. This is in agreement with pervious theoretical [51] and experimental results [53]. The quenching of the average magnetization was explained due to antiferromagnetic order in the iron-rich core.
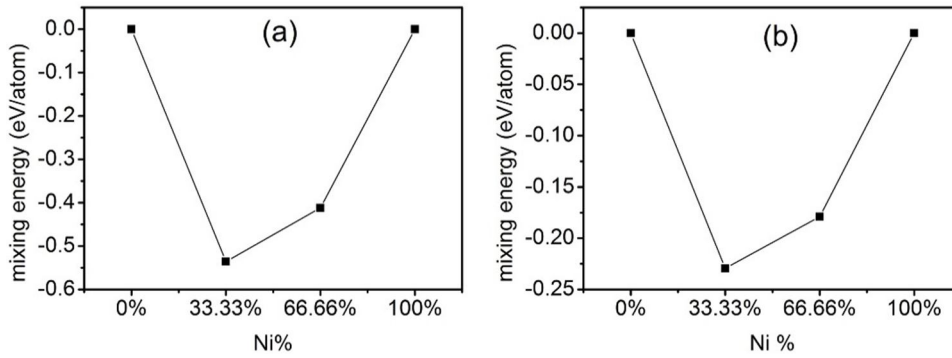
FIG. 1. Mixing energy of Ni_nFe_{3-n} clusters *versus* Ni concentration (%) for (a) linear and (b) triangular clusters.
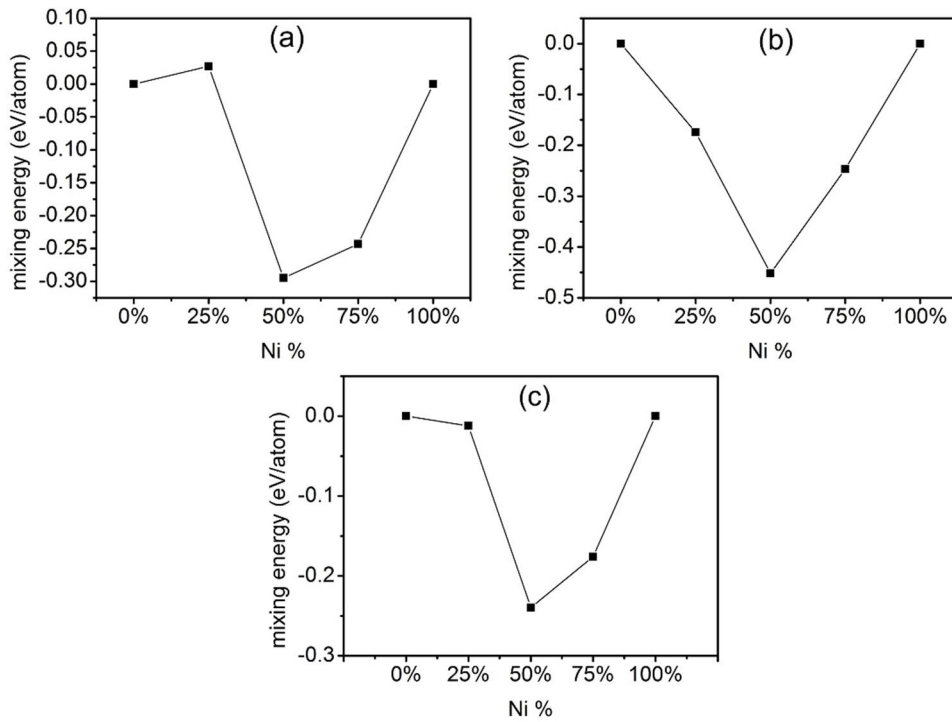

FIG. 2. Mixing energy of Ni_nFe_{4-n} clusters *versus* Ni concentration (%) for (a) square, (b) rhombic and (c) tetrahedral clusters.
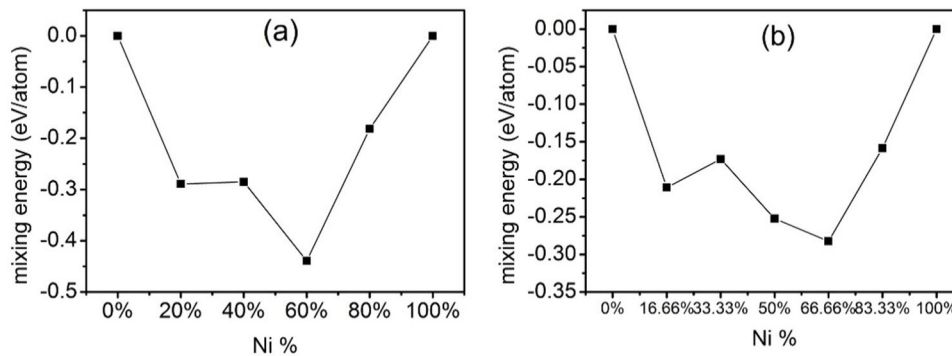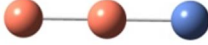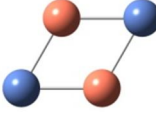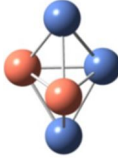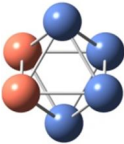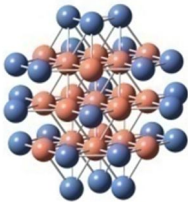

FIG. 3. Mixing energy of Ni_nFe_{N-n} (N=5, 6) clusters *versus* Ni concentration (%) for (a) trigonal bipyramidal and (b) octahedron clusters.

TABLE 2. The structures of the most stable Ni_nFe_{N-n} isomers with N = 2 to 6 and N = 43, symmetry, magnetic moment per atom and bond lengths.

N	System	Ni%	Structure	Symmetry	Magnetic moment per atom (μ_B/atom)	Bond length (Å)		
						Fe-Fe	Fe-Ni	Ni-Ni
2	FeNi	50%		$C_{\infty v}$	5.05	-	2.03	-
3	Fe$_2$Ni	33.3%		$C_{\infty v}$	2.67	2.13	2.09	-
4	Fe$_2$Ni$_2$	50%		D_{2h}	2	2.14	2.27	-
5	Fe$_2$Ni$_3$	60%		C_{2v}	2	2.41	2.25 and 2.30	2.39
6	Fe$_2$Ni$_4$	66.7%		C_{2v}	2	2.41	2.28 - 2.30	3.34 - 2.37
43	Fe$_{19}$Ni$_{24}$	55.8%		O_h (fcc)	1.73	2.56 - 2.63	2.33 and 2.40	2.48

The colors of the atoms are blue for Ni atoms and orange for Fe atoms.

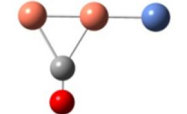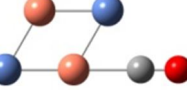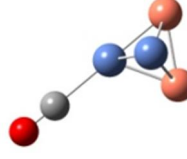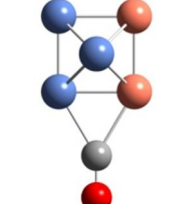### 3.3 The Adsorption of CO on the Most Stable Ni_nFe_{N-n} Clusters

The adsorption of CO is investigated on the most stable isomers of the selected Ni_nFe_{N-n} clusters (n = 2 to 6) as well as on Fe$_{19}$Ni$_{24}$ cluster. The values are then compared with the adsorption on bare Fe and Ni clusters. The adsorption of CO molecule is investigated at different high-symmetry sites: top, bridge and hollow sites (except for n = 2). In case of Ni-Fe dimer, we studied the adsorption of CO on Ni and Fe atoms of Ni-Fe dimer. We found that the adsorption of CO on Ni atom (where C is bound to Ni) is the most stable structure of Ni-Fe dimer with an adsorption energy of 1.708 eV. The Ni-Fe bond length of 2.19 Å is larger than in the case without adsorption (2.03 Å). The Ni-C is 1.76 Å and the C–O bond length is 1.16 Å, which is larger than that of free CO gas (1.128 A). The total magnetic moment is found to be 4.0 μ_B, which is smaller than that of bare Ni-Fe dimer (5.05 μ_B) due to the adsorption of CO molecule. In addition, the adsorption frequency of the adsorbed CO on Ni-Fe is 1981.43 cm^{-1}. This value is less than the vibrational frequency of the free CO molecule (2102.82 cm^{-1}), which is ascribed to the weakening of CO bond due to adsorption. In addition, the adsorption energy of CO on Ni-Fe bond is 1.708 eV, which is less than the adsorption energy on bare Ni dimer (1.891 eV), while it is more than that on bare Fe dimer (1.366 eV), see Table 3. Table 3 includes

the most stable adsorption sites of CO on the most stable Ni_nFe_{N-n} clusters and adsorptions energies, as well as the adsorption energies on the corresponding Ni and Fe bare clusters with the same structures. The top position on Fe atom is found to be the most stable site of CO adsorption on Ni_nFe_{N-n} clusters (N=3 and N=4). However, the most stable site is at the top position of Ni atom for the case of N=5. On the other hand, the bridge site between Ni and Fe atoms is the most stable site in the case of N=6. The larger cluster of N=43, however, shows that the hollow site is the most stable site for CO adsorption with an adsorption energy of 1.817 eV (Fig. 4). This is in agreement with previous studies using DFT and cluster expansion methods, where the active site on bimetallic Fe-Ni nanoparticles has most of Ni atoms neighboring to CO adsorbate [41]. However, a previous DFT study has shown that the most stable site of CO adsorption on FeNi(111) surface is the intermediate position between bridge Ni site and top Fe [42]. The adsorption energies on bare Fe clusters are much larger than those on bare Ni clusters (Table 3), in agreement with a previous theoretical study that used both DFT and cluster expansion methods [41]. In addition, the adsorption energies of CO on the bimetallic Ni_nFe_{N-n}, except for FeNi dimer, are lower than the adsorption energies of CO on the corresponding bare Fe clusters with the same structure (Table 3 and Fig. 5). This means that the adsorption of CO decreases upon alloying in Ni_nFe_{N-n} clusters, which decreases the poisoning by CO and correspondingly increases the MOR efficiency. In addition, locating the Fe atoms in the hidden core decreases the adsorption of CO on Ni_nFe_{N-n} clusters. The presence of Fe atoms in the core with Ni atoms at the surface was previously confirmed by theoretical [41, 50, 51] and experimental [52] studies.

TABLE 3. The adsorption energies of CO on the most stable Ni_nFe_{N-n} clusters at the most stable sites and the adsorption energies on the corresponding Ni and Fe bare clusters (N = 2 to 6).

N	structure	Adsorption energy E_{ads} (eV)		
		Ni_nFe_{N-n} clusters	Ni bare clusters	Fe bare clusters
2		1.708	1.891	1.366
3		2.281	1.538	2.645
4		1.870	2.094	2.567
5		2.278	2.443	4.736
6		2.047	1.948	3.753

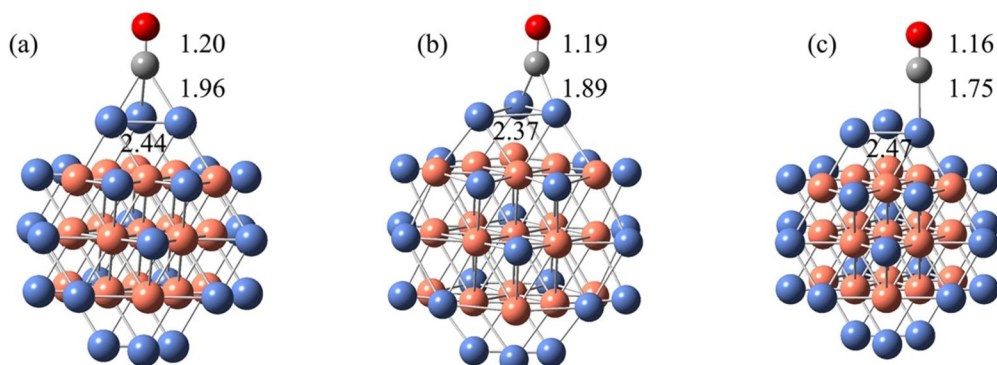The colors of the atoms are blue for Ni atoms, orange for Fe atoms. gray for carbon atom and red for oxygen atom.

FIG. 4. The adsorption of CO on Fe$_{19}$Ni$_{24}$ cluster at (a) the hollow site (b) the bridge and (c) the top site. The colors of the atoms are blue for Ni atoms, orange for Fe atoms. gray for carbon atom and red for oxygen atom.
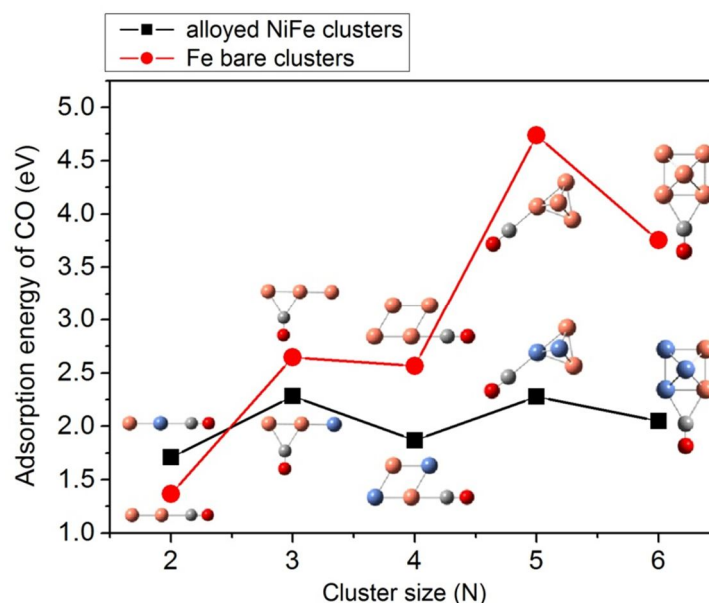

FIG. 5. The adsorption energies of CO on the most stable Ni_nFe_{N-n} clusters at the most stable sites and the adsorption energies on the corresponding Fe bare clusters (N = 2 to 6).

4. Conclusion

DFT calculations were performed to investigate the structural, energetic and magnetic properties of bimetallic Ni_nFe_{N-n} clusters (n = 2 to 6 and N = 43). The mixing energies of bimetallic clusters have negative values, which indicates that alloyed clusters are more stable than Fe and Ni bare clusters. The most stable isomers have C$_{\infty v}$, D$_{2h}$ for small alloyed clusters with N = 3, 4, respectively and C$_{2v}$ for both N = 5 and 6. All small alloyed clusters exhibit a high-spin ground state. However, Fe$_{19}$Ni$_{24}$ large cluster exhibits a lower magnetization per atom due to antiferromagnetic coupling of iron core atoms, inconsistent with previous studies.

The adsorption energies of CO on most stable alloyed bimetallic Ni_nFe_{N-n} isomers are found to be lower than those on the corresponding Fe bare clusters. This indicates a decrease of CO poisoning and an increase of MOR activity upon alloying. The presence of Fe atoms in the core with Ni atoms at the surface of large Fe$_{19}$Ni$_{24}$ clusters is found to lower the contact with CO and this leads to a decrease of CO poisoning, in agreement with previous experimental and theoretical studies of iron-core shape of Ni-Fe nano-particles. The most stable adsorption sites of CO on the most stable Ni_nFe_{N-n} isomers are the top sites on Fe atom for N = 3 and N = 4, whereas the top site on Ni atom was found to be the most stable site for N = 5. However, the bridge position between Ni and Fe atoms and the hollow sites are the most stable sites for the cases of N = 6 and N = 43, respectively.

Acknowledgement

Declaration of Interest Statement

The authors confirm that there are no competing interests regarding the materials/work discussed in this manuscript.

References

[1] Liu, H. and Hernandez, E.S., J. Nanosci. Nanotechnol., 14 (2014) 1533.

[2] Wang, S.C. and Ehrlich, G., Phys. Rev. Lett., 93 (2004) 17.

[3] Martin, T.P., Phys. Rep., 273 (1996) 199.

[4] Apsel, S.E., Emmert, J.W., Deng, J. and Bloomfield, L.A., Phys. Rev. Lett., 76 (1996) 1441.

[5] Kakar, S., Björneholm, O., Weigelt, J., De Castro, A.R.B., Tröger, L., Frahm, R., Möller, T., Knop, A. and Rühl. E., Phys. Rev. Lett., 78 (1997) 1675.

[6] Alcántara Ortigoza, M. and Rahman, T.S., Phys. Rev. B - Condens. Matter Mater. Phys., 77 (2008) 195404.

[7] Zhong, W., Liu, Y. and Zhang, D., J. Mol. Model., 18 (2012) 3051.

[8] Maheswari, S., Karthikeyan, S., Murugan, P., Sridhar, P. and Pitchumani, S., Phys. Chem. Chem. Phys., 14 (2012) 9683.

[9] Gonella, F., Mattei, G., Mazzoldi, P., Sada, C., Battaglin, G. and Cattaruzza, E., Appl. Phys. Lett., 75 (1999) 55.

[10] Pal, U., Sanchez Ramirez, J.F., Liu, H.B., Medina, A. and Ascencio, J.A., Appl. Phys. A Mater. Sci. Process, 79 (2004) 79.

[11] Ascencio, J.A., Liu, H.B., Pal, U., Medina, A. and Wang, Z.L., Microsc. Res. Tech., 69 (2006) 522.

[12] Luo, J., Maye, M.M., Kariuki, N.N., Wang, L., Njoki, P., Lin, Y., Schadt, M., Naslund, H.R. and Zhong, C.J., Catal. Today, 99 (2005) 291.

[13] Luo, J., Njoki, P.N., Lin, Wang, L. and Zhong, C.J., Electrochem. Commun., 8 (2006) 581.

[14] Maye, M.M., Kariuki, N.N., Luo, J., Han, L., Njoki, P., Wang, L., Lin, Y., Naslund, H.R. and Zhong, C.J., Gold Bull., 37 (2004) 217.

[15] Luo, J., Maye, M.M., Petkov, V., Kariuk, N.N., Wang, L., Njoki, P., Mott, D., Lin, Y. and Zhong, C.J., Chem. Mater., 17 (2005) 3086.

[16] Landon, P., Collier, P.J., Carley, A.F., Chadwick, D., Papworth, A.J., Burrows, A., Kiely, C.J. and Hutchings, G.J., Phys. Chem. Chem. Phys., 5 (2003) 1917.

[17] Venezia, A.M., La Parola, V., Nicolì, V. and Deganello, G., J. Catal., 212 (2002) 56.

[18] Benedetti, A., Bertoldo, L., Canton, P., Goerigk, G., Pinna, F., Riello, P. and Polizzi, S., Catal. Today, 49 (1999) 485.

[19] Lemire, C., Meyer, R., Shaikhutdinov, S. and Freund, H.J., Angew. Chemie - Int. Edn., 43 (2004) 118.

[20] Donsì, F., Williams, K.A. and Schmidt, L.D., Ind. Eng. Chem. Res., 44 (2005) 3453.

[21] González, M.J., Hable, C.T. and Wrighton, M.S., J. Phys. Chem. B, 102 (1998) 9881.

[22] Cho, S.J. and Ryoo, R., Catal. Letters, 97 (2004) 71.

[23] Gu, Y., Wu, G., Hu, X.F., Chen, D.A., Hansen, T., zur Loye, H.C. and Ploehn, H.J., J. Power Sources, 195 (2010) 425.

[24] Datta, J., Singh, S., Das, S. and Bandyopadhyay, N.R., Bull. Mater. Sci., 32 (2009) 643.

[25] Roth, C., Benker, N., Theissmann, R., Nichols, R.J. and Schiffrin, D.J., Langmuir, 24 (2008) 2191.

[26] Bauer, A., Gyenge, E. L. and Oloman, C. W., J. Power Sources 167 (2007), 281.

[27] Tao, F., Grass, M.E., Zhang, Y., Butcher, D.R., Renzas, J.R., Liu, Z., Chung, Y.J., Mun, B.S., Salmeron, M. and Somorjai, G.A., Science, 322 (2008) 932.

[28] Lim, B. and Xia, Y., Angew. Chemie - Int. Edn., 50 (2011) 76.

[29] Koenigsmann, C., Santulli, A.C., Gong, K., Vukmirovic, M.B., Zhou, W.P., Sutter, E., Wong, S.S. and Adzic, R.R., J. Am. Chem. Soc., 133 (2011) 9783.

[30] Wang, L., Nemoto, Y. and Yamauchi, Y., J. Am. Chem. Soc., 133 (2011) 9674.

[31] Sanchez, S.I., Small, M.W., Zuo, J.M. and Nuzzo, R.G., J. Am. Chem. Soc., 131 (2009) 8683.

[32] Wang, L. and Yamauchi, Y., Chem. - An Asian J., 5 (2010) 2493.

[33] Murugadoss, A., Okumura, K. and Sakurai, H., J. Phys. Chem. C, 116 (2012) 26776.

[34] Sheth, P.A., Neurock, M. and Smith, C.M., J. Phys. Chem. B, 109 (2005) 12449.

[35] Zea, H., Lester, K., Datye, A.K., Rightor, E., Gulotty, R.,Waterman, W. and Smith, M., Appl. Catal. A, Gen., 282 (2005) 237.

[36] Candelaria, S.L., Bedford, N.M., Woehl, T.J., Rentz, N.S., Showalter, A.R., Pylypenko, S., Bunker, B.A., Lee, S., Reinhart, B., Ren, Y., Ertem, S.P., Coughlin, E.B., Sather, N.A., Horan, J.L., Herring, A.M. and Greenlee, L.F., ACS Catal., 7 (2017) 365.

[37] Jiang, Q., Jiang, L., Hou, H., Qi, J., Wang, S. and Sun, G., J. Phys. Chem. C, 114 (2010) 19714.

[38] Spendelow, J.S. and Wieckowski, A., Phys. Chem. Chem. Phys., 9 (2007) 2654.

[39] Chen, G., Dai, Z., Bao, H., Zhang, L., Sun, L., Shan, H., Liu, S. and Ma, F., Electrochim. Acta, 336 (2020) 135751.

[40] Liu, J., Lucci, F.R., Yang, M., Lee, S., Marcinkowski, M.D., Therrien, A.J., Williams, C.T., Sykes, E.C. H. and Flytzani-Stephanopoulos, M., J. Am. Chem. Soc., 138 (2016) 6396.

[41] Teeriniemi, J., Melander, M., Lipasti, S., Hatz, R. and Laasonen, K., J. Phys. Chem. C, 121 (2017) 1667.

[42] Canto, G., Dzib, L., Lanz, C., Juan, A., Brizuela, G. and Simonetti, S., Mol. Phys., 110 (2012) 113.

[43] Kohn, W. and Sham, L.J., Phys. Rev., 140 (1965) A1133.

[44] Perdew, J.P., Burke, K. and Ernzerhof, M., Phys. Rev. Lett., 77 (1996) 3865.

[45] Giannozzi, P., Baroni, S., Bonini, N., Calandra, M., Car, R., Cavazzoni, C., Ceresoli, D., Chiarotti, G.L., Cococcioni, M., Dabo, I., Corso, A.D., Gironcoli, S.D., Fabris, S., Fratesi, G., Gebauer, R., Gerstmann, U., Gougoussis, C., Kokalj, A., Lazzeri, M., Martin-Samos, L., Marzari, N., Mauri, F., Mazzarello, R., Paolini, S., Pasquarello, A., Paulatto, L., Sbraccia, C., Scandolo, S., Sclauzero, G., Seitsonen, A.P., Smogunov, A., Umari, P. and Wentzcovitch, R.M., J. Phys. Condens. Matter, 21 (2009) 395502.

[46] Methfessel, M. and Paxton, A.T., Phys. Rev. B, 40 (1989) 3616.

[47] Cheng, H.P. and Ellis, D.E., J. Chem. Phys., 94 (1991) 3735.

[48] Rao, B.K., Ramos de Debiaggi, S. and Jena, P., Phys. Rev. B - Condens. Matter Mater. Phys., 64 (2001) 244181.

[49] Nakazawa, T., Igarashi, T., Tsuru, T. and Kaji, Y., Comput. Mater. Sci., 46 (2009) 367.

[50] Sahoo, S., Rollmann, G. and Entel, P., Phase Transitions, 79 (2006) 693.

[51] Guirado-López, R.A. and Aguilera-Granja, F., J. Phys. Chem. C, 112 (2008) 6729.

[52] Parks, E.K., Kerns, K.P. and Riley, S.J., Chem. Phys., 262 (2000) 151.

[53] Li, X.G., Chiba, A. and Takahashi, S., J. Magn. Magn. Mater., 170 (1997) 339.